J Toxicol Pathol 2024; 37: 69–82

Original Article

Combination of pathological, biochemical and behavioral evaluations for peripheral neurotoxicity assessment in isoniazid-treated rats

Akane Kashimura[1,2*], Satomi Nishikawa[1], Yuhei Ozawa[1], Yui Hibino[1], Takashi Tateoka[1], Mao Mizukawa[1,2], Hironobu Nishina[1], Tetsuya Sakairi[1], Takanori Shiga[2], Naoyuki Aihara[2], and Junichi Kamiie[2*]

[1] Safety Research Laboratories, Sohyaku, Innovative Research Division, Mitsubishi Tanabe Pharma Corporation, Shonan Health Innovation Park, 2-26-1 Muraoka-Higashi, Fujisawa-shi, Kanagawa 251-8555, Japan
[2] Laboratory of Veterinary Pathology, School of Veterinary Medicine, Azabu University, 1-17-71 Fuchinobe, Chuo-ku, Sagamihara-shi, Kanagawa 252-5201, Japan

Abstract: In drug development, assessment of non-clinical peripheral neurotoxicity is important to ensure human safety. Clarifying the pathological features and mechanisms of toxicity enables the management of safety risks in humans by estimating the degree of risk and proposing monitoring strategies. Published guidelines for peripheral neurotoxicity assessment do not provide detailed information on which endpoints should be monitored preferentially and how the results should be integrated and discussed. To identify an optimal assessment method for the characterization of peripheral neurotoxicity, we conducted pathological, biochemical (biomaterials contributing to mechanistic considerations and biomarkers), and behavioral evaluations of isoniazid-treated rats. We found a discrepancy between the days on which marked pathological changes were noted and those on which biochemical and behavioral changes were noted, suggesting the importance of combining these evaluations. Although pathological evaluation is essential for pathological characterization, the results of biochemical and behavioral assessments at the same time points as the pathological evaluation are also important for discussion. In this study, since the measurement of serum neurofilament light chain could detect changes earlier than pathological examination, it could be useful as a biomarker for peripheral neurotoxicity. Moreover, examination of semi-thin specimens and choline acetyltransferase immunostaining were useful for characterizing morphological neurotoxicity, and image analysis of semi-thin specimens enabled us to objectively show the pathological features. (DOI: 10.1293/tox.2023-0094; J Toxicol Pathol 2024; 37: 69–82)

Key words: peripheral neurotoxicity, nerve fiber degeneration, isoniazid, vitamin B6, neurofilament light chain, rat

Introduction

Drug-induced peripheral neuropathy has often been reported in non-clinical and clinical studies during drug development. Accurate assessment of peripheral neurotoxicity in nonclinical studies is important to ensure human safety. An accurate assessment to characterize the pathophysiology and elucidate the mechanism of peripheral neurotoxicity enables the management of safety risks in humans by estimating the degree of risk and proposing monitoring strategies. Published guidelines (Organisation for Economic Co-operation and Development [OECD] guidance and review articles) for peripheral neurotoxicity assessment do not provide detailed information on which endpoints should be monitored preferentially and how the results should be integrated and discussed[1–5]. In the early stages of drug development, the observation items for evaluating neurotoxicity may not be designed for screening studies to select better candidates. A battery for evaluating neurotoxicity is sometimes included in general toxicology studies; however, it is often difficult to set a complete panel of measurement parameters and observation items for test articles with unknown toxicological profiles. Therefore, it is important to detect possible neurotoxicity in candidates at an early stage for further development of selected candidates. Non-clinical neurotoxicity assessment, particularly for peripheral neurotoxicity, is complicated by the following issues: (1) lack of established peripheral neurotoxicity biomarkers (BMs), (2)

Received: 9 August 2023, Accepted: 8 December 2023
Published online in J-STAGE: 29 December 2023
*Corresponding authors: A Kashimura
(e-mail: kashimura.akane@ma.mt-pharma.co.jp);
J Kamiie (e-mail: kamiie@azabu-u.ac.jp)
(Supplementary material: refer to PMC https://www.ncbi.nlm.nih.gov/pmc/journals/1592/)

lack of clarity regarding which behavioral evaluation should be conducted, (3) lack of established standard methods for objective measurement of pathologic toxicity features, and (4) difficulties in choosing the appropriate necropsy time points.

Humoral BMs can be used in both clinical and nonclinical studies in drug development, as required. A highly sensitive BM is useful for monitoring neurotoxicity in humans[6]. The neurofilament light chain (Nf-L) is a protein component of nerve cells that is established as a humoral BM of axonal injury, reflecting central neurodegenerative diseases and traumatic brain injuries[7–9]. In recent years, Nf-L has attracted attention as a humoral BM for peripheral nerve injury[6, 10]. Some studies have detected a significant increase in serum Nf-L levels in rats with peripheral nerve injury[11–13].

Isoniazid (INH), an anti-tuberculosis drug, induces peripheral neurotoxicity owing to vitamin B6 (VB6) deficiency[14]. The main circulating forms of VB6 are pyridoxal (PL) and its active form, pyridoxal phosphate (PLP), which can be detected in the plasma. According to review articles, INH inhibits pyridoxal phosphokinase (PDXK), an enzyme that converts PL to PLP, resulting in PLP depletion and peripheral neuropathy[14, 15]. However, the association between serum PLP levels and neurotoxicity is not well established[16]. It is difficult to detect a uniform decrease in plasma VB6 levels in humans because of the large variation in the dietary intake of VB6 among individuals, and no study in laboratory animals has compared the time course of changes in plasma VB6 levels with toxic changes. Peripheral neurotoxicity from INH treatment is due to distal axonal degeneration[17, 18], and several reports have provided detailed pathological examinations of morphological changes over time[17, 19, 20]. However, whether these changes due to PLP deficiency are mainly located in sensory or motor neurons has not been clearly determined[16, 21–23]. In clinical practice, these changes may initially occur in sensory nerves, but later signs of motor dysfunction may appear[24, 25].

To determine an optimal assessment method for the characterization of peripheral neurotoxicity, we conducted pathological, biochemical, and behavioral evaluations of INH-treated rats. In this study, we aimed to effectively narrow down the neurotoxicity endpoints in the early stages of drug development.

Materials and Methods

Animals

Five-week-old male Sprague-Dawley (Crl:CD) rats were purchased from Charles River Laboratories Japan (Kanagawa, Japan) and used at 6 weeks of age. INH (Cat No. 13377, Sigma-Aldrich, St. Louis, MO, USA) was dissolved in 0.5% (w/v) methylcellulose - 0.3% (w/v) Tween 80 solution and administered orally for 3 days at 0 (vehicle control), 250 (low dose), and 500 (high dose) mg/kg/day. Day 1 was defined as the first day of dosing. The animals were euthanized by exsanguination under deep anesthesia with isoflurane inhalation on days 4, 9, or 30. The dose and the timing of necropsy were determined based on the results of a preliminary study, in which animals were dosed with INH at 300, 500, and 1,000 mg/kg/day, over a similar time course. The 1,000 mg/kg/day group showed severe body weight loss, and the 500 mg/kg/day showed sufficient peripheral neurotoxicity. Details of the group dose and necropsy schedules are listed in Table 1. All animals were fasted in the evening before sacrifice (days 3, 8, and 29). Blood was collected from the posterior vena cava of the animals under anesthesia for each examination. Necropsies, including macroscopic observation of the external surface and organs in the thoracic and abdominal cavities, were performed. After transcardiac perfusion with 4% paraformaldehyde, the brain, spinal cord (including the dorsal root ganglion [DRG]), sciatic, tibial, and saphenous nerves were excised. Tissues were immersed in 10% neutral-buffered formalin, and part of the sciatic nerve was fixed in 2.5% glutaraldehyde for electron microscopy. All procedures were endorsed by the Institutional Animal Care and Use Committee of the test facility and performed in accordance with animal welfare and Mitsubishi Tanabe Pharma Corporation's internal rules for proper conduct of animal experiments.

Endpoints in living animals

All animals were observed for clinical signs immediately after dosing during the dosing period and once daily during other periods. Body weight and food consumption were measured on days 1–9, 11, 14, 18, 21, 25, and 29.

As behavioral evaluations, a thermal sensation test (hot plate method) and detailed symptom observation (selected items from the modified Irwin's test: locomotor activity,

Table 1. Composition of the Animal Groups

Group No.	Necropsy day	Isoniazid dose (mg/kg/day)	Dose volume (mL/kg/day)	Dose concentration (mg/mL)	Number of animals (Animal #)
1	Day 4	0	5	0	5 (10101-10105)
2	Day 4	250	5	50	5 (10201-10205)
3	Day 4	500	5	100	5 (10301-10305)
4	Day 9	0	5	0	5 (10401-10405)
5	Day 9	250	5	50	5 (10501-10505)
6	Day 9	500	5	100	5 (10601-10605)
7	Day 30	0	5	0	5 (10701-10705)
8	Day 30	250	5	50	5 (10801-10805)
9	Day 30	500	5	100	5 (10901-10905)

body posture, ataxic gait, abnormal gait, abdominal muscle tone, trunk muscle tone, limb muscle tone, ipsilateral flexor reflex, grip strength, pinna reflex, corneal reflex, and pain reaction[26, 27]) were performed on days-1, 3, 8, and 18. The tests were not performed on day 29 because there were no changes on days 8 and 18. On days 4, 5, 6, 9, and 30, the ipsilateral flexor reflexes of the hindlimbs were assessed (Fig. 1). For the thermal sensation test, after a rat had 2 minutes of acclimation on a hot plate at room temperature, we measured the latency (seconds) to perform avoidance behavior when it was placed on a hot plate at approximately 53°C. The test was performed in duplicate to confirm the reproducibility. Avoidance behavior was judged by the observer based on the manifestations of licking, rearing, tapping, or jumping. A latency ≥10 seconds in both of the duplicate measurements was recorded as an abnormality because the latencies on day-1 and in the control group were <10 seconds.

Hematology and blood chemistry

For hematological analysis, blood samples were collected in anticoagulant (EDTA-2K)-coated tubes. The following parameters were measured with an automated analyzer (Automated Hematology Analyzer XT-2000iV, Sysmex Corporation, Kobe, Japan): erythrocyte count, hemoglobin concentration, hematocrit, mean corpuscular volume, mean corpuscular hemoglobin, mean corpuscular hemoglobin concentration, red cell distribution width, reticulocyte count and ratio, platelet count, mean platelet volume, leukocyte count, and differential leukocyte count and ratio (lymphocytes, neutrophils, monocytes, eosinophils, and basophils).

For the blood chemistry analysis, serum was obtained from the collected blood samples. The following items were measured with an automated analyzer (Hitachi Automatic Analyzer LABOSPECT 006, Hitachi High-Tech Corporation, Tokyo, Japan): aspartate aminotransferase, alanine aminotransferase, glutamate dehydrogenase (GLDH), alkaline phosphatase, total bilirubin (Tbil), direct bilirubin (Dbil), indirect bilirubin (calculated from Tbil and Dbil), total bile acid, urea nitrogen (UN), creatinine (CRE), glucose, total cholesterol, triglycerides, total protein, albumin/globulin ratio, calcium, inorganic phosphorus, sodium, potassium, and chloride (Cl).

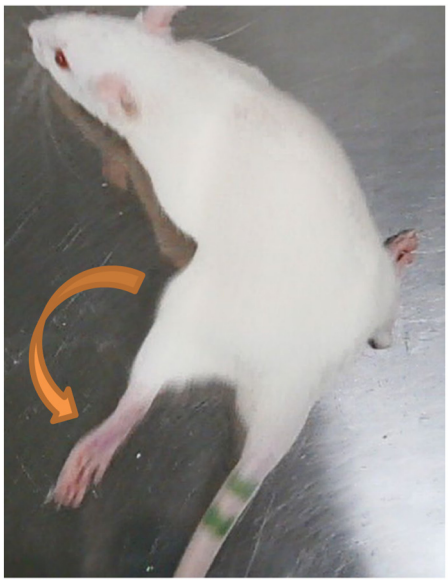

Fig. 1. The ipsilateral flexor reflex of the hindlimbs. When the hindlimb is extended caudally, the flexor reflex normally causes the hindlimb to flex back into original position.

Serum Nf-L measurement

Serum was obtained from collected blood samples. Serum samples from to 3–5 animals per group (except for group 8) were used to obtain the Nf-L concentration. Serum Nf-L concentrations were measured using a Simoa HD-X analyzer (Quanterix, Billerica, MA, USA) with a Simoa NF-light V2 Advantage Kit (Cat No. 104073, Quanterix) according to the manufacturer's instructions. For measurement validation, the accuracy of the calibration curve, concentration of quality control (QC) samples, intra- and inter-assay reproducibility, and dilution parallelism were confirmed. For the measurement batch, data that met the criteria for the accuracy of the calibration curve and concentration of QC samples were adopted.

Plasma VB6 measurement

Plasma was obtained from the blood samples collected in anticoagulant (EDTA-2K)-coated tubes. To prepare the standard solutions, serial dilutions of pyridoxal hydrochloride for PL, pyridoxal 5-phosphate monohydrate for PLP, and heptafluorobutyric acid were purchased from Sigma-Aldrich. The concentrations of the prepared standard solutions are shown within the calibration curve in Supplementary Table 1. The internal standard (IS) solutions were prepared by diluting stock solutions of pyridoxal hydrochloride methyl-D3 and pyridoxal 5′-phosphate methyl-D3 purchased from Buchem B.V. (Apeldoorn, NL, USA) to 100 and 75 nM, respectively. Plasma samples, trichloroacetic acid solution, and IS solution of the stable isotope for each analyte were mixed to precipitate the plasma proteins. The centrifuged supernatant was used for analysis. Standard solutions were processed in the same manner and used as calibration curve standards.

PL and PLP were measured individually by liquid chromatography–tandem mass spectrometry (LC-MS/MS) system. The system was composed of a Prominence series (Shimadzu Corporation, Kyoto, Japan), Nexera X2 series (Shimadzu Corporation), and Qtrap 4500 system (Sciex, Framingham, MA, USA). Analyst, version 1.6.2 (AB Sciex) was used to control the instrument and data acquisition. The PL was separated on an Acquity HSS-T3 guard column (1.8 µm, 2.1 mm × 5 mm, Waters, Milford, MA, USA) and an Acquity HSS-T3 analytical column (1.8 µm, 2.1 mm × 100 mm, Waters). PLP was separated on an Acquity HSS-T3 guard column (1.8 µm, 2.1 mm × 5 mm; Waters) and an InertSustain C18 analytical column (1.8 µm, 2.1 mm ×

100 mm; GL Sciences Inc., Tokyo, Japan). Both the analytes were eluted using a gradient mobile phase system consisting of two components. The mass spectrometer was operated in positive MRM mode with a dwell time of 100 ms. The analyte-specific settings are shown in Supplementary Table 1.

Histopathological examination of formalin-fixed paraffin-embedded (FFPE) sections

Fixed tissues were dehydrated, embedded in paraffin, and stained with hematoxylin and eosin (HE) using routine methods. HE-stained slides of the brain, spinal cord (including the DRG), sciatic nerve, tibial nerve, and saphenous nerve were prepared for microscopic examination. The peripheral nerves were prepared longitudinally. In addition, for the sciatic nerve, Luxol Fast Blue (LFB)-Bodian staining was performed for identification of axons and myelin sheaths. The sections were then examined under a microscope.

For immunohistochemistry, sciatic nerve sections of three representative animals were selected and used to characterize the nerve fiber degeneration and recovery process observed in the HE sections from each of the following groups: Group 4 (received INH 0 mg/kg/day; scheduled sacrifice on day 9), Group 6 (received INH 500 mg/kg/day; scheduled sacrifice on day 9), and Group 9 (received INH 500 mg/kg/day; scheduled sacrifice on day 30). After deparaffinization, immunohistochemistry was performed with an anti-choline acetyltransferase (ChAT) antibody (Cat No. Ab178850, Abcam, Cambridge, UK, 1:1,000 dilution) and anti-Nf-L antibody (Cat No. M0762, Agilent Technologies, Santa Clara, CA, USA, 1:500 dilution) and an anti-ionized calcium-binding adapter molecule 1 (Iba1) antibody (Cat No. 019-19741, Fujifilm Wako, Osaka, Japan, 1:2,000 dilution) using an automated staining device (HISTOSTAINER 48A, Nichirei Biosciences Inc., Tokyo, Japan) in accordance with the manufacturer's instructions. Heat-induced epitope retrieval was performed with citrate or Tris-EDTA buffer and blocked with a protein-blocking buffer (Block Ace Powder, Cat No. UKB 80, KAC), in accordance with standard procedures. Sections were incubated with the primary antibody for 1 h and then with a secondary antibody for 30 min at room temperature. Immunoreactivity was detected and visualized by performing a peroxidase-diaminobenzidine (DAB) reaction (Peroxidase Stain DAB Kit [Brown Stain], Nacalai Tesque, Kyoto, Japan) before counterstaining the sections with hematoxylin.

Histopathological examination using semi-thin sections

For the sciatic nerves of all animals, toluidine blue (TB)-stained semi-thin sections were prepared and examined using light microscopy. For image analysis, whole digital slide images were obtained using virtual microscopy (Aperio AT2, Leica Biosystems, Wetzlar, Germany); then, using HALO image analysis software (v3.64134.166, Indica Labs, Albuquerque, NM, USA) and its Axon module, histopathological features of neuron fibers were analyzed and quantified for all animals. The following parameters were measured: axon count, total area (axon, nerve fiber, myelin, and total tissue areas), average diameter (axon and nerve fiber diameters), and average area (axon, nerve fiber, and myelin areas). A valid analysis method to clarify the histopathological features is histogram analysis, which can show the distribution of nerve fibers with morphological differences for each individual. To clarify the histopathological features, we used the G-ratio (proportion of axonal diameter in the nerve fiber diameter) data[28] and performed a histogram analysis for two representative animals selected from each of the following groups: Group 4 (received INH 0 mg/kg/day; scheduled sacrifice on day 9) and Group 6 (received INH 500 mg/kg/day; scheduled sacrifice on day 9). To verify the accuracy of the image recognition of nerve fibers by the software, the positive predictive value and sensitivity were calculated by counting the number of nerve fibers and visually comparing the actual stained images with the nerve fibers recognized by the software. The 125 μm × 125 μm squares were extracted randomly from three sites/animal, and nerve fibers were counted visually.

Ultrastructural examination

To clarify the ultrastructural features of nerve fiber degeneration, ultrathin sections were prepared from the sciatic nerves of two animals per group according to the conventional method. The sections were then stained with uranyl acetate and examined. The nerve fiber findings were compared with those of the control group and photographs were obtained using a transmission electron microscope (JEM-1400, JEOL Ltd., Tokyo, Japan).

Statistical analysis

Dunnett's multiple comparison test was performed on hematological parameters, blood chemistry parameters, serum Nf-L levels, and plasma VB6 levels. All significance levels were two-sided at the 5% level.

Results

Endpoints in living animals including behavioral findings

There were no marked changes in clinical signs or necropsy findings in any of the groups. Dose-dependent body weight loss or suppression of body weight gain was observed during the dosing period and was associated with decreased food consumption. However, the changes recovered promptly after the completion of dosing (Fig. 2).

In the behavioral assessment, a delay from placement on a hot plate to avoidance behavior was observed in 2 of the 15 animals in the high-dose group on day 3. No abnormalities were observed on day 8. Mild hyporeflexia of the ipsilateral flexor muscle of the hindlimb was observed in 3 of the 15 animals in the high-dose group on day 4. One of these animals showed changes on day 5. No changes were observed in the behavioral evaluation conducted from day 6 onward (Table 2).

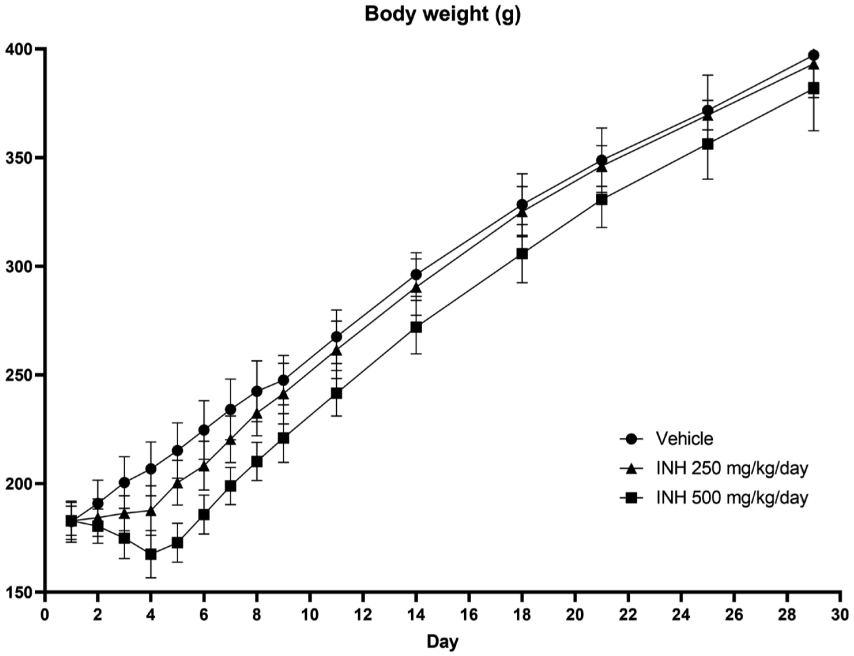

Fig. 2. Average body weight from day 1 to day 29. Dose-dependent weight loss or suppression of weight gain was observed until day 4 (the day after the end of isoniazid [INH] dosing); however, body weight recovered after day 5. Error bars indicate standard deviation.

Hematology and blood chemistry

Hematological analysis showed that the reticulocyte count decreased in a dose-dependent manner on day 4 and increased on day 9 in the high-dose group (Fig. 3). The decrease on day 4 was considered a transient change associated with a decrease in body weight during the dosing period, with the increase on day 9 being a rebound effect.

Blood chemistry analysis revealed the following findings on day 4 (Fig. 3): Cl levels increased slightly in the high-dose group and were associated with a decrease in body weight. Mild increases in the GLDH, UN, and CRE levels were observed, suggesting transient hepatorenal dysfunction. INH is known to cause various injuries due to VB6 deficiency, including hepatic and renal disorders. However, these changes were not considered to interfere with the evaluation of peripheral neurotoxicity because the event was transient and the results had returned to normal by day 9 and thereafter.

Serum Nf-L levels

Serum Nf-L levels were measured to confirm the utility of Nf-L as a humoral BM (Fig. 4 and Table 2). On day 4, serum Nf-L levels were increased markedly in a dose-dependent manner, but the increase was not statistically significant because of inter-individual variability. On day 9, the levels were increased with less variation than on day 4, and the increase was statistically significant in the high-dose group. On day 30, the levels of both treatment groups were comparable to those of the control group.

Plasma concentrations of PL and PLP

To investigate the possible relationship between VB6 levels and neurotoxicity caused by INH treatment, plasma concentrations of PL, as well as its activated phosphorylated form PLP, reflecting the tissue stores of VB6[16], were measured. A marked dose-dependent decrease in both the PL and PLP levels was observed on day 4; however, no decrease was observed after day 9 (Fig. 5 and Table 2). The decrease in plasma VB6 levels rapidly recovered after the dosing period.

Histopathological findings of FFPE sections and semi-thin sections

In the histopathological examination of the FFPE sections, nerve fiber degeneration was observed in each peripheral nerve, indicating neuropathy caused by INH (Tables 2 and 3). There were no significant differences in the degree of change between the sciatic, tibial, and saphenous nerves. Nerve fiber degeneration was observed only sporadically in the high-dose group on day 4, and was most marked and observed at a high frequency on day 9 (Fig. 6A). On day 30, nerve fiber degeneration had recovered, while sporadic macrophages between nerve fibers stained positive for Iba1 and had foamy cytoplasm (Fig. 6A and 6B). Macrophage infiltration was considered indicative of the scavenging ability of macrophages to remove damaged axons and/or myelin components. In HE and LFB-Bodian staining, nerve fiber degeneration was recognized as “digestion chambers” with fragmented axons and spherules derived from the myelin sheath at sites where axons had disappeared (Fig. 6C). No significant changes were observed in the brain, spinal cord, and DRG.

Table 2. Summary of the Results of Each Evaluation

			Results									Discussion	
			Vehicle	INH low	INH high	Vehicle	INH low	INH high	Vehicle	INH low	INH high	Usefulness of the endpoints	
Assessment		Findings	Days 3–5			Days 8–9			Day 30			Advantages	Disadvantages
Behavioral assessment	Ipsilateral flexor reflex (one of the Irwin's test) [a]	Mild hyporeflexia of the hindlimb	-	-	P (3/15) [b]	-	-	-	-	-	-	- High sensitivity: Behavioral abnormalities not detected in general clinical signes were detected - Easy to include in toxicity studies: Easy to assess and low stress on animals	- Causes of abnormal movements cannot be identified
	Thermal sensitivity test (hotplate method) [c]	Delayed time from placement on a hot plate to evading behavior	-	-	P (2/15)	-	-	-	NA	NA	NA	- High sensitivity: Behavioral abnormalities not detected in general clinical signes were detected	- Difficult to judge by subjective observation - Too much time for acclimatization and evaluation - Unable to detect sensory abnormalities other than thermal stimuli
Assessment			Day 4			Day 9			Day 30			Advantages	Disadvantages
Bioanalysis	Serum Nf-L (pg/mL)		17.6 ± 6.30 (n=4)	143 ± 180 (n=5) d	813 ± 909 (n=4) d	7.79 ± 0.88 (n=3)	23.1 ± 21.2 (n=5)	128 ± 69.6 (n=5)**	5.99 ± 1.21 (n=3)	NA	10.1 ± 4.05 (n=5)	- High sensitivity and early detectivity: Even minor changes difficult to note by pathology became high value - Less invasivity	- High inter-individual variability - Less specificity: Nf-L is a constituent protein in nerve tissue and cannot specify which nerve tissue is damaged
	Plasma PL (nM)		611 ± 183 (n=5)	106 ± 48.2 (n=5)***	60.1 ± 23.7 (n=5)***	583 ± 59.8 (n=5)	624 ± 219 (n=5)	563 ± 195 (n=5)	415 ± 92.3 (n=5)	481 ± 125 (n=5)	395 ± 55.0 (n=5)	- Useful for mechanistic discussion	- Difficult to measure: Some endogenous molecules - Unable to determine what to measure if a mechanistic hypothesis cannot be developed
	Plasma PLP (nM)		803 ± 131 (n=5)	137 ± 44.9 (n=5)***	35.8 ± 8.41 (n=5)***	759 ± 37.8 (n=5)	637 ± 75.4 (n=5)* e	727 ± 92.2 (n=5)	796 ± 121 (n=5)	822 ± 116 (n=5)	734 ± 118 (n=5)		
Assessment		Findings	Day 4			Day 9			Day 30			Advantages	Disadvantages
Pathology	FFPE specimens, HE stain (sciatic nerve)	Degeneration of nerve fiber	-	-	+ (3/5)	-	+ (4/5), ++ (1/5)	++ (3/5), +++ (2/5)	-	-	-	- Wide evaluation area: especially longitudinal	- Inability to distinguish detailed features
		Appearance of phagocyte	-	-	-	-	-	-	-	-	+ (2/5), ++ (3/5)	- Able to compare changes in multiple nerves	
	Semi-thin specimens, TB stain (sciatic nerve)	Myelin ovoid, appearance	-	+ (1/5)	+ (2/5)	-	+ (3/5)	++ (4/5), +++ (1/5)	-	-	-	- Pathologic characterization: Axons or myelin sheaths - High sensitivity: Findings detected at low dose on day 4	- Small evaluation area
		Shrunken axon	-	-	-	-	-	+ (5/5)	-	-	-		
		Increase, Schwann cell	-	-	-	-	-	+ (2/5)	-	-	-		
		Increase, small myelinated fiber	-	-	-	-	-	-	-	-	+ (2/5)		

Advantages and disadvantages identified from the results are noted. Toxicologically significant changes are highlighted in gray. Descriptions in parentheses: number of animals with findings/number of animals examined. INH low: isoniazid 250 mg/kg/day for 3 days; INH high: isoniazid 500 mg/kg/day for 3 days; Nf-L: neurofilament light chain; PL: pyridoxal; PLP: pyridoxal phosphate; FFPE: formalin-fixed paraffin-embedded; HE: hematoxylin and eosin; TB: toluidine blue; -: no noteworthy findings; P: present; +: mild; ++: moderate; +++: severe; NA: not appreciable. Dunnett's multiple comparison test: *p<0.05 vs. control, **p<0.01 vs. control, ***p<0.001 vs. control. a: Ipsilateral flexor reflex was examined on days 3–6, 8–9, and 30. b: Mild hyporeflexia of the hind limb was noted in 3 of 15 animals on day 4, and in 1 of 10 animals on day 5. It was not noted on day 3 and after day 6. c: Thermal sensitivity test was performed on days 3 and 8. d: The increases were considered toxicologically significant treatment-related changes, because multiple animals were noted at a clearly high level that does not occur normally, regardless of no statistical significance. e: The decrease was not considered a treatment-related change, because it was a mild decrease and not noted in the high-dose group, regardless of statistical significance.

On immunohistochemistry with an anti-ChAT antibody, a toxicologically relevant positive reaction was not observed in the degenerated nerve fibers (Fig. 7). ChAT is a marker of the cholinergic nerves (autonomic and motor nerves). This result suggests that axonal degeneration occurs mainly in the sensory nerves of the peripheral nerves.

Light microscopic observations of TB-stained semi-thin specimens were also performed. In animals with severe pathology, blue-stained myelin ovoids and morphological variability (unequal size or irregular shape) of each nerve fiber were frequently observed (Fig. 8A). Myelin ovoids are caused by winding proliferation of the myelin sheath, which occurs after the axons are damaged and lost. This finding was also observed on day 4 in the low-dose group, without any findings in the FFPE specimens (Table 3). The unequal size of nerve fibers is thought to result from changes such as the expansion of axons associated with axonal injury (considered to be caused by the proliferation of intracellular organelles), enlargement of nerve fibers caused by reactive changes in the myelin sheath, and the appearance of small nerve fibers for regeneration.

Image analysis of semi-thin sections

We used the HALO software to distinguish axons from myelin sheaths and to quantify the diameter and area of each nerve fiber. Based on the obtained values, we evaluated the G-ratio (axonal diameter/nerve fiber diameter) using a histogram as a distribution of the number of nerve fibers[28]. In the histogram of the animals received INH 500 mg/kg/day compared with that of the vehicle-treated animals, the increased myelin ovoids in the sections of the INH-treated animals showed a marked increase in the G-ratio 0 value. In addition, the variability in nerve fibers was shown as a decreased G-ratio distribution and a slight increase in the G-ratio 0.6–0.8 value (Fig. 8B). The validity of image recognition was demonstrated by visually counting nerve fibers and calculating the positive predictive value and sensitivity of nerve fiber recognition. Both the positive predictive value and sensitivity were greater than 90% (Supplementary Table 2).

Ultrastructural findings

Ultrastructural examination revealed a time-course change in the axonal degeneration (Fig. 9). On day 4, the disruption of axons and myelin sheaths was observed as an early sign of axonal injury, and axonal disintegration-associated myelin ovoids were occasionally present. On day 9, axonal degeneration, disruption of the myelin sheath, and myelin ovoid formation with loss of axons were observed in many nerve fibers. Enlargement of Schwann cells, hypermyelination, and an increase in small myelinated fibers were observed as reactive changes. On day 30, the frequency of small nerve fibers with thin myelin sheaths, indicative of their repair processes, increased.

Discussion

To find an optimal assessment method for the characterization of peripheral neurotoxicity, we conducted a pathological, biochemical and behavioral evaluations in INH-treated rats and assessed the combination of the results. Necropsy was conducted at three time points: immediately after the dosing period, on day 4, when pathological changes were still very slight; on day 9, when pathological changes were marked; and on day 30, when reversibility could be assessed. Peripheral neurotoxicity may be delayed, and reversibility is an important aspect of the assessment. There was a discrepancy between the time course of pathological changes and biochemical and behavioral test results (Table 3), suggesting the importance of assessing these relationships over time.

In particular, the usefulness of Nf-L as a peripheral neurotoxic BM is strongly suggested for the detection of nerve fiber injury. Serum Nf-L levels were higher on day 4 than on day 9, the time of the most prominent peripheral nerve injury, suggesting that more Nf-L leaked during the early phase of injury. On day 4, serum Nf-L levels were also high in the low-dose group, with minor changes that were

Table 3. Histopathological Findings of Formalin-fixed Paraffin-embedded Sections for Each Peripheral Nerve

Findings	Day 4			Day 9			Day 30		
Tissues	Vehicle	INH low	INH high	Vehicle	INH low	INH high	Vehicle	INH low	INH high
Degeneration of nerve fiber									
Sciatic nerve	-	-	+ (3/5)	-	+ (4/5), ++ (1/5)	++ (3/5), +++ (2/5)	-	-	-
Tibial nerve	-	-	+ (2/5)	-	+ (2/5), ++ (3/5)	+++ (5/5)	-	-	+ (1/5)
Saphenous nerve	-	-	+ (2/5)	-	+ (3/5), ++ (2/5)	++ (1/5), +++ (4/5)	-	-	-
Appearance of phagocyte									
Sciatic nerve	-	-	-	-	-	-	-	-	+ (2/5), ++ (3/5)
Tibial nerve	-	-	-	-	-	-	-	-	+ (4/5)
Saphenous nerve	-	-	-	-	-	-	-	-	+ (2/5)

Descriptions in parentheses: number of animals with findings/number of animals examined. INH low: isoniazid 250 mg/kg/day for 3 days; INH high: isoniazid 500 mg/kg/day for 3 days. -: no noteworthy findings; +: mild; ++: moderate; +++: severe.

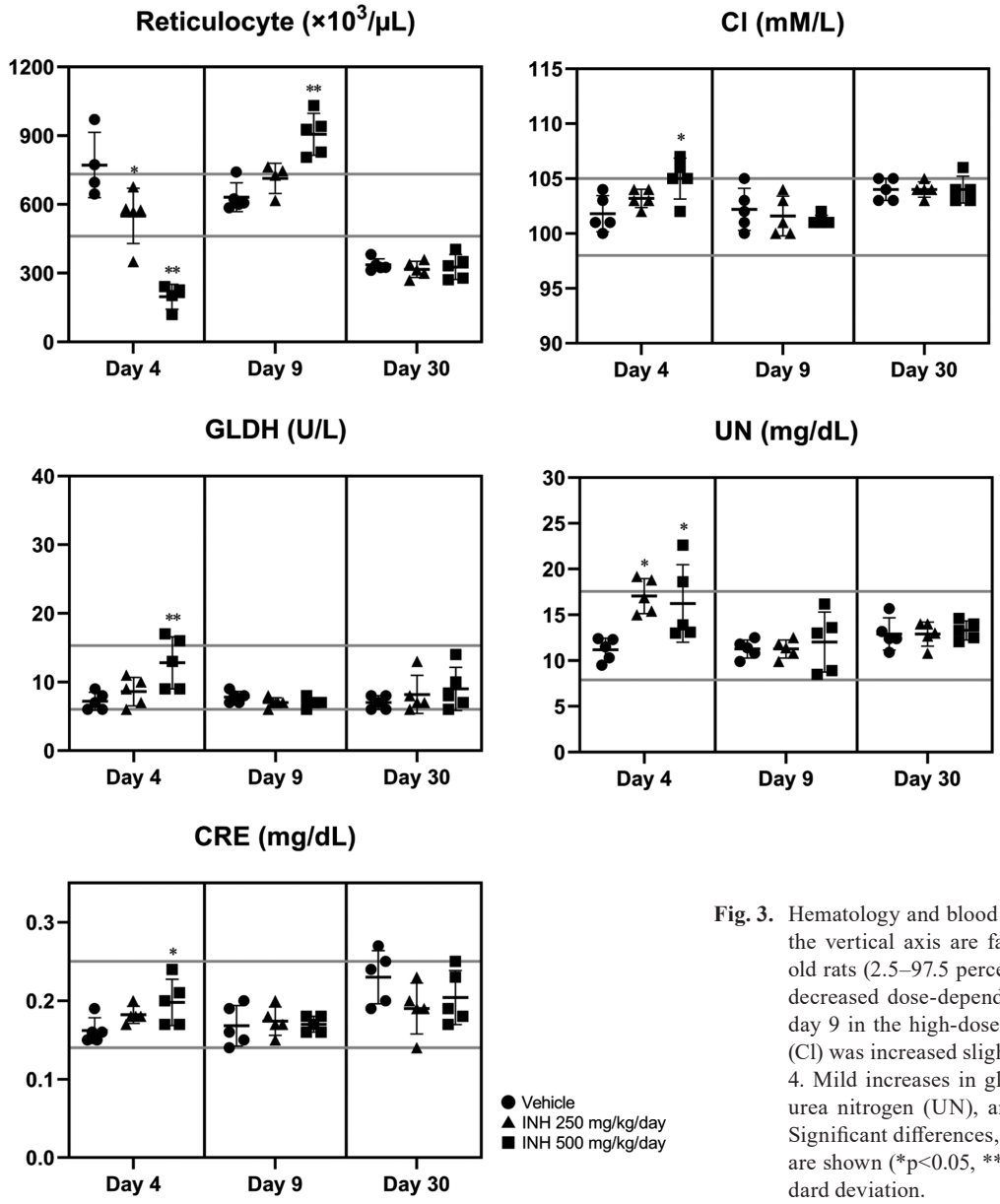

Fig. 3. Hematology and blood chemistry at necropsy. Values on the vertical axis are facility data from normal 7-week-old rats (2.5–97.5 percentile, n=109). Reticulocytes were decreased dose-dependently on day 4 and increased on day 9 in the high-dose isoniazid (INH) group. Chloride (Cl) was increased slightly in the high-dose group on day 4. Mild increases in glutamate dehydrogenase (GLDH), urea nitrogen (UN), and creatinine (CRE) were noted. Significant differences, compared with the vehicle group, are shown (*p<0.05, **p<0.01). Error bars indicate standard deviation.

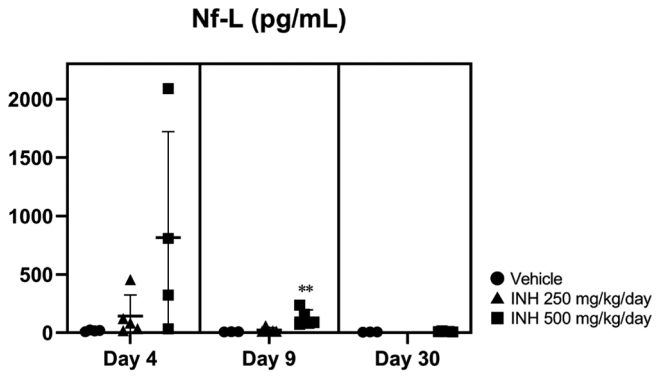

Fig. 4. Serum concentrations of neurofilament light chain (Nf-L) at necropsy. By day 4, Nf-L levels increased markedly in a dose-dependent manner, but they were not statistically significant because of interindividual variability. On day 9, the Nf-L level were increased with less variation than that on day 4, and the increase was statistically significant in the high-dose isoniazid (INH) group. On day 30, the levels of both treatment groups were not increased. Significant differences, compared with the vehicle group, are shown (**p<0.01). Error bars indicate standard deviation.

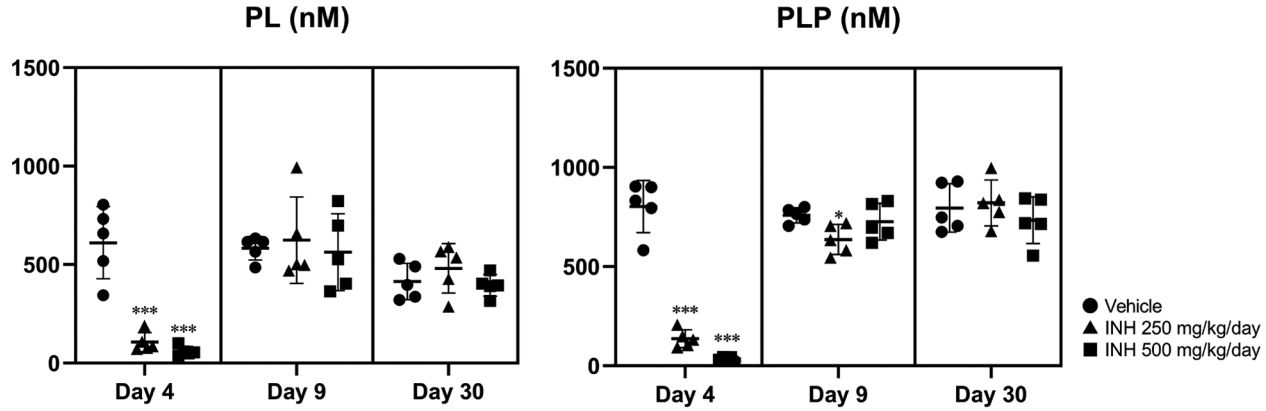

Fig. 5. Plasma concentrations of pyridoxal (PL) and pyridoxal phosphate (PLP) at necropsy. On day 4, both levels of isoniazid (INH) treatment groups were markedly reduced in a dose-dependent manner. After day 9, both levels were unchanged compared with the vehicle group. Significant differences, compared with the vehicle group, are shown (*$p<0.05$, ***$p<0.001$). Error bars indicate standard deviation.

difficult to detect in FFPE sections, suggesting that Nf-L is a useful humoral BM that can sensitively detect minor lesions that cannot be detected in FFPE sections. We assumed that serum Nf-L levels would increase concurrently with pathological changes because Nf-L is a neuronal protein component. In previous studies, serum Nf-L levels were high when peripheral nerve lesions induced by hyperpyridoxine and paclitaxel were prominent[12, 13], and gradually increased during vincristine and cisplatin dosing and peaked at the final time point[11, 12]. Interestingly, our results showed that the time of the highest peak in Nf-L was earlier than that of the pathological changes. Serum Nf-L measurement is non-invasive and useful for monitoring toxicity in humans. Even at an early stage, when it is difficult to detect clear morphological changes and the degree of the lesions is likely to differ among individuals, changes can be detected even with a small sample size, because serum Nf-L levels are markedly high due to nerve injury. As Nf-L cannot distinguish between neuronal damage in the central nervous system (CNS) and the peripheral nervous system, concomitant evaluation of the CNS is required. In this study, no marked changes were observed in the pathological evaluation of the brain and spinal cord, and we believe that the increase in serum Nf-L levels was caused by peripheral nerve injury.

In another bioanalysis, plasma PL and PLP levels were measured. Both decreased by day 4 and recovered by day 9, when nerve fiber degeneration was prominent. Chua *et al*. reported that PLP conversion of VB6 incorporated into nerve tissue occurs mainly in nerve cell bodies, and that PLP is transported to axons and used for metabolism[17]. The distal axon of the neuron is susceptible to the effects of PLP deficiency, which can lead to nerve fiber degeneration in the long peripheral nerve axons[17]. Therefore, it is likely that it took time for the pathological changes to appear due to the processes of decreased PLP concentration in nerve tissue, transport, and metabolic disorders, which occur after the decrease in plasma PLP levels. Changes in plasma PL and PLP levels at an early stage are useful markers for the early prediction of subsequent peripheral nerve injury. We often cannot determine what to measure if there is no mechanistic hypothesis for toxicity, and some endogenous molecules are difficult to measure. However, the measurement of biological substances related to mechanistic hypotheses can provide a useful rationale for discussing toxicity mechanisms.

In the behavioral evaluation, evaluation of the ipsilateral flexor reflex was considered useful. It can detect behavioral abnormalities that cannot be detected by general clinical observations. Although the incidence was low, this change was considered to be related to neurotoxicity rather than a decline the animals' body weight. In our previous study (data not shown), 6-week-old Sprague-Dawley rats administered 25% restricted feeding for 3 days showed marked body weight loss, emaciation, and low reticulocyte count, with no effects on activity or behavior. Ipsilateral flexor reflex evaluation would be easy to include in general toxicity studies and could be evaluated daily because it is easy to check and places little stress on the animals. Although abnormalities were also detected in the thermal sensory stimulation test, it was considered that it would be difficult to incorporate this in routine toxicity evaluation because it was difficult to judge the change by subjective observation and it took a long time for acclimation and evaluation. Another disadvantage is that the effect target is often unknown in general toxicity studies, unlike in pharmacology studies; therefore, sensory abnormalities other than thermal stimulation may not be detected. The small number of animals with changes in both evaluations was considered to be due to possible differences in severity between animals and the possibility that symptoms may not appear if there are more than a certain number of nerve fibers with residual function.

In the pathological evaluation, TB-stained semi-thin specimens were useful for morphological characterization of peripheral neurotoxicity. Semi-thin specimens can be used to evaluate the details of the changes, including the location and whether axons or myelin sheaths are present. Even if semi-thin specimens are not available, LFB-Bodian

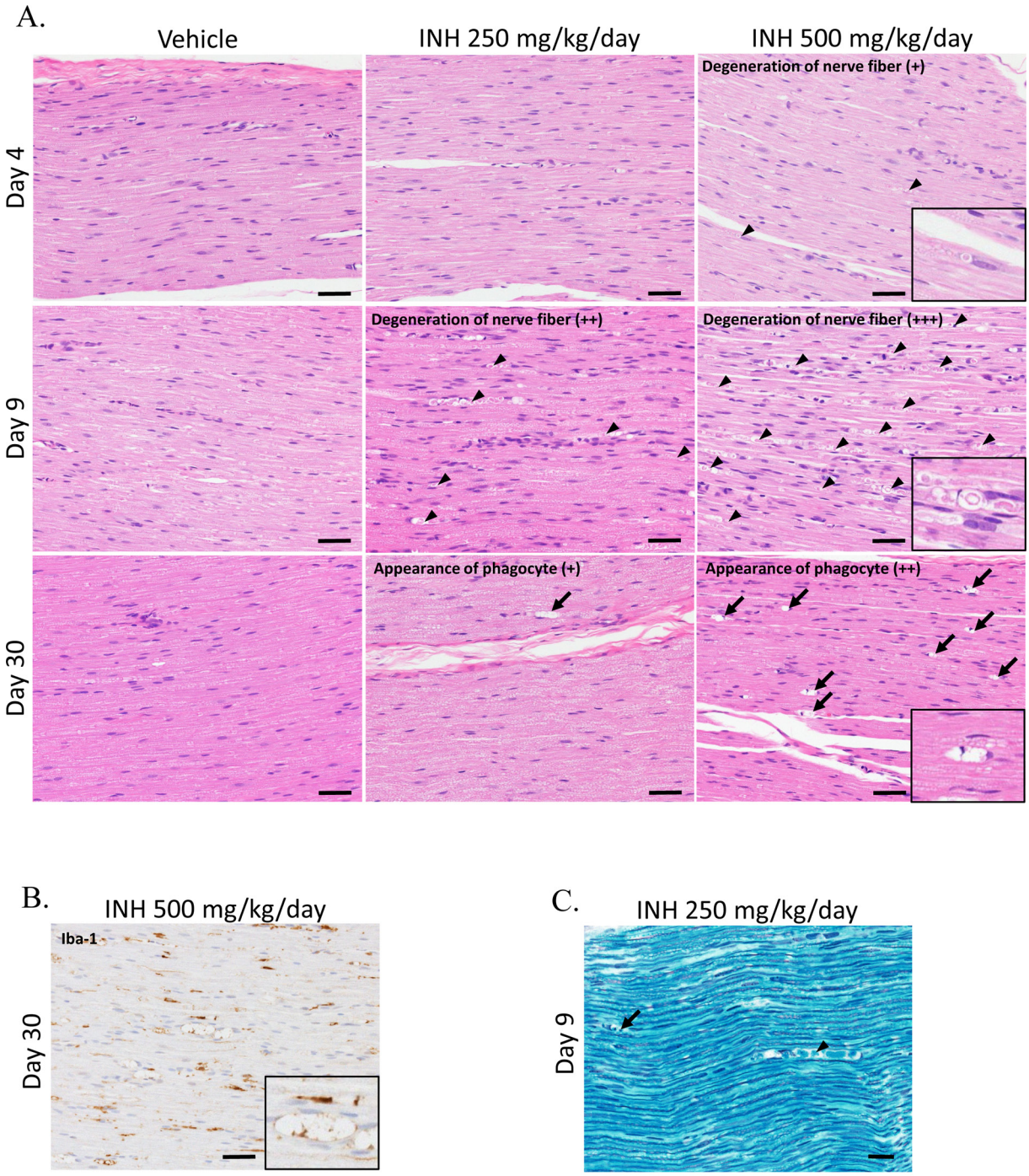

Fig. 6. Histopathology of the sciatic nerve in formalin-fixed paraffin-embedded sections. A: Hematoxylin and eosin staining. In isoniazid (INH) treatment groups, nerve fiber degeneration was observed in some nerve fibers on day 4, became most significant by day 9, and recovered by day 30 (arrowhead). The frequency of the change increased in a dose-dependent manner. On day 30, foamy cells were observed (arrow). Scale bar=50 µm. B: Immunohistochemistry for Iba1. The foamy cells were positive for Iba1. Scale bar=50 µm. C: Luxol Fast Blue-Bodian staining of the sciatic nerve on day 9 in the low-dose group. Nerve fiber degeneration was observed to be "digestion chambers" with axon fragmentation (arrow) and spherules derived from the myelin sheath (arrowhead). Scale bar=20 µm.

staining can distinguish between axons and myelin sheaths to some extent. The assessment of semi-thin specimens was more sensitive than that of FFPE specimens because an increase in myelin ovoids was detected even in the low-dose group on day 4, when no findings were observed in FFPE specimens. However, the assessment of semi-thin specimens must be combined with that of FFPE specimens because the evaluation area in semi-thin specimens is very narrow.

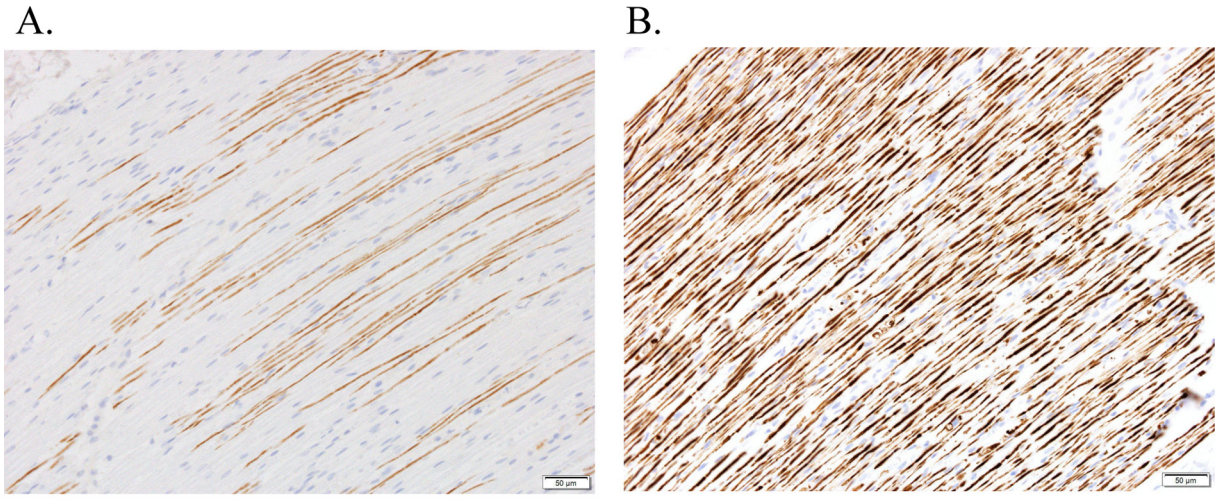

Fig. 7. Immunohistochemistry for choline acetyltransferase (ChAT) in the sciatic nerve in formalin-fixed paraffin-embedded sections. The images on day 9 in the high-dose group are shown. ChAT was positive for axons of motor neurons (A). Nf-L was positive in all axons, and numerous degenerated nerve fibers are observed (B). No nerve fiber degeneration was observed in the ChAT-positive nerve fibers. Scale bar=50 µm.

In image analysis, the pathological features were presented as data that are easily understood by non-pathologists by showing the G-ratio as a histogram. Since pathological evaluation is subjective, it is desirable to use an objective index. While the usefulness of image analysis for pathological evaluation has been frequently reported not only in the clinical field but also in the non-clinical toxicity field in recent years[29–31], this study is one example that demonstrates the usefulness of image analysis for neurotoxicity. For image analysis, we suggest that data showing the validity of the image recognition used for the analysis should be handled as validation data. In drug development, it is particularly important to demonstrate the validity of image analysis when obtaining data to be used for new drug applications, and standardization of the validation of image analysis will be required in the future[32].

ChAT immunostaining of FFPE specimens revealed no nerve fiber degeneration in the ChAT-positive motor neurons. The saphenous nerve, which contains only somatosensory fibers in rats[33], was affected in a manner similar to that of the sciatic nerve. These results suggest that INH-induced peripheral neurotoxicity occurs primarily in the sensory nerves, although it is unclear whether INH-induced peripheral neurotoxicity is primarily located in the sensory or motor nerves[16, 21–23]. This is consistent with clinical signs that begin with sensory abnormalities in the feet[24, 25]. Differentiation of the motor and sensory nerves is important for characterizing pathology and investigating monitoring methods in humans. Although ChAT is mainly used for staining nerve cell bodies in the CNS, our results showed that ChAT can also objectively distinguish motor and sensory neurons in peripheral nerves in tissue sections.

In this study, we assessed peripheral neurotoxicity in INH-treated rats using a combination of evaluations to determine the optimal assessment method for the characterization of peripheral neurotoxicity. There was a discrepancy between the time points of marked pathological changes and the changes in biochemical and behavioral assessments, suggesting the importance of setting multiple necropsy time points and combining each evaluation. Although pathological evaluation is essential for pathological characterization, the results of biochemical and behavioral assessments at the same time points as the pathological evaluation are valuable. In this study, using an INH-induced peripheral neuropathy rat model, we found that serum Nf-L measurement could detect changes earlier than pathology, indicating it would be very useful as a BM for peripheral neurotoxicity. Moreover, the observation of semi-thin specimens and ChAT immunostaining were useful for characterizing morphological neurotoxicity, and image analysis of semi-thin specimens enabled us to objectively show pathological features. In order to generalize our approach, further evaluation in any peripheral neurotoxic model will be required.

Disclosure of Potential Conflicts of Interest: The authors declare that there are no conflicts of interest.

Acknowledgment: The authors would like to thank Katsuya Fujiki for the technical efforts and ingenuity in the pathological evaluations. We are also grateful to the members of the Mitsubishi Tanabe Pharma Corporation safety research laboratories for their cooperation in promoting this study.

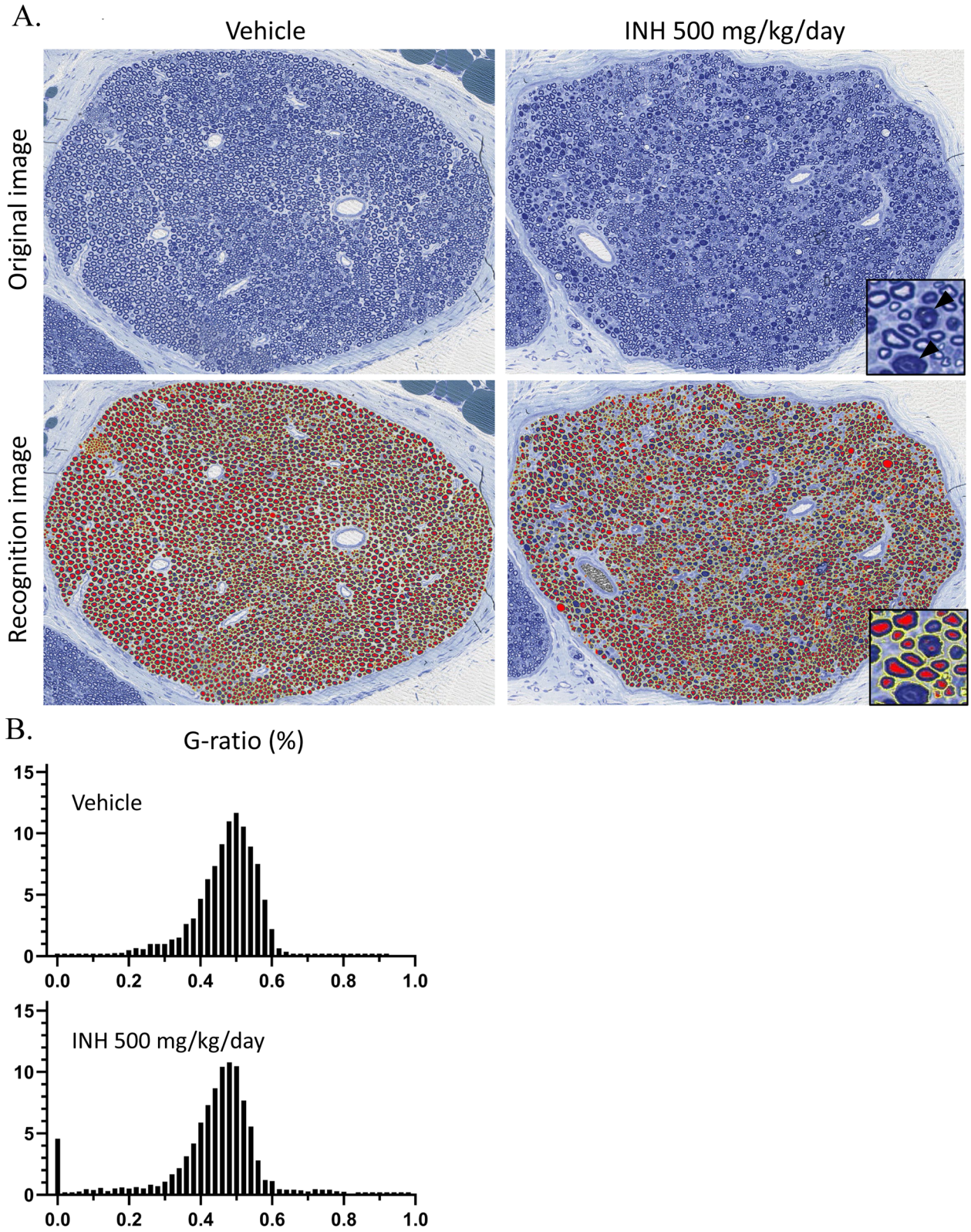

Fig. 8. A: Representative toluidine blue-stained semi-thin specimens of the sciatic nerve on day 9. The sciatic nerve of a rat treated with isoniazid (INH) 500 mg/kg/day showed a marked increase in myelin ovoids (arrowhead), and size differences in nerve fiber diameter. The images after recognition by the axon module of the HALO software were also presented. Nerve fibers are surrounded by yellow lines, and axons are painted red. B: The G-ratio (axon diameter/nerve fiber diameter) was calculated for each nerve fiber, and its distribution was shown as a histogram. In the histogram of a rat treated with INH 500 mg/kg/day compared to that of a vehicle received rat, a marked increase in the G-ratio 0 value was noted. In addition, the variability in nerve fibers was shown as a decrease of the G-ratio distribution and a slight increase in the G-ratio 0.6–0.8 value.

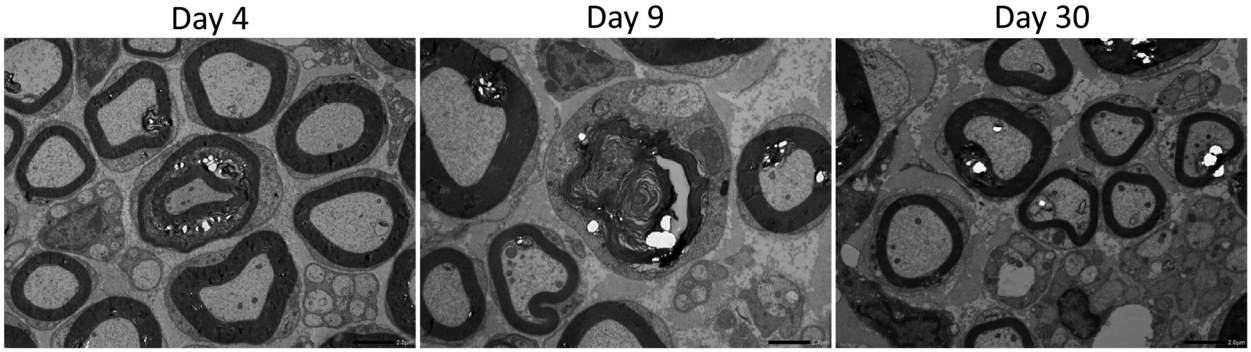

Fig. 9. Ultrastructural observation of the sciatic nerve in the high-dose isoniazid group. Representative images are shown. On day 4, disruption of axon and myelin sheath were observed as early signs of axonal injury. On day 9, axonal degeneration, disruption of myelin sheath, and myelin ovoid formation were observed in many nerve fibers, accompanied by enlargement of Schwann cells. On day 30, the frequency of small nerve fibers with thin myelin sheaths was increased. Scale bar=2 µm.

References

1. OECD. Guidance document for neurotoxicity testing. OECD Environment, Health and Safety Publications Series on Testing and Assessment, No. 20. Paris. 2004.
2. OECD. Neurotoxicity study in rodents. OECD Guideline for the Testing of Chemicals, No. 424. Paris. 1997.
3. EPA. Neurotoxicity screening battery. Health Effects Test Guidelines, OPPTS 870.6200. Washington DC. 1998.
4. Bolon B, Krinke G, Butt MT, Rao DB, Pardo ID, Jortner BS, Garman RH, Jensen K, Andrews-Jones L, Morrison JP, Sharma AK, and Thibodeau MS. STP position paper: recommended best practices for sampling, processing, and analysis of the peripheral nervous system (nerves and somatic and autonomic ganglia) during nonclinical toxicity studies. Toxicol Pathol. **46**: 372–402. 2018. [Medline] [CrossRef]
5. Bruna J, Alberti P, Calls-Cobos A, Caillaud M, Damaj MI, and Navarro X. Methods for in vivo studies in rodents of chemotherapy induced peripheral neuropathy. Exp Neurol. **325**: 113154. 2020. [Medline] [CrossRef]
6. Bonomo R, and Cavaletti G. Clinical and biochemical markers in CIPN: a reappraisal. Rev Neurol (Paris). **177**: 890–907. 2021. [Medline] [CrossRef]
7. Coppens S, Lehmann S, Hopley C, and Hirtz C. Neurofilament-light, a promising biomarker: analytical, metrological and clinical challenges. Int J Mol Sci. **24**: 11624. 2023.
8. Alcolea D, Beeri MS, Rojas JC, Gardner RC, and Lleó A. Blood biomarkers in neurodegenerative diseases: implications for the clinical neurologist. Neurology. **101**: 172–180. 2023. [Medline] [CrossRef]
9. Arslan B, and Zetterberg H. Neurofilament light chain as neuronal injury marker—what is needed to facilitate implementation in clinical laboratory practice? Clin Chem Lab Med. **61**: 1140–1149. 2023. [Medline] [CrossRef]
10. Rossor AM, and Reilly MM. Blood biomarkers of peripheral neuropathy. Acta Neurol Scand. **146**: 325–331. 2022. [Medline] [CrossRef]
11. Meregalli C, Fumagalli G, Alberti P, Canta A, Carozzi VA, Chiorazzi A, Monza L, Pozzi E, Sandelius Å, Blennow K, Zetterberg H, Marmiroli P, and Cavaletti G. Neurofilament light chain as disease biomarker in a rodent model of chemotherapy induced peripheral neuropathy. Exp Neurol. **307**: 129–132. 2018. [Medline] [CrossRef]
12. Meregalli C, Fumagalli G, Alberti P, Canta A, Chiorazzi A, Monza L, Pozzi E, Carozzi VA, Blennow K, Zetterberg H, Cavaletti G, and Marmiroli P. Neurofilament light chain: a specific serum biomarker of axonal damage severity in rat models of chemotherapy-induced peripheral neurotoxicity. Arch Toxicol. **94**: 2517–2522. 2020. [Medline] [CrossRef]
13. Sano T, Masuda Y, Yasuno H, Shinozawa T, Watanabe T, and Kakehi M. Blood neurofilament light chain as a potential biomarker for central and peripheral nervous toxicity in rats. Toxicol Sci. **185**: 10–18. 2021. [Medline] [CrossRef]
14. Badrinath M, and John S. Isoniazid toxicity. 2022, from StatPearls Publishing website: https://www.ncbi.nlm.nih.gov/books/NBK531488.
15. Hadtstein F, and Vrolijk M. Vitamin B-6-induced neuropathy: exploring the mechanisms of pyridoxine toxicity. Adv Nutr. **12**: 1911–1929. 2021. [Medline] [CrossRef]
16. Reddy P. Preventing vitamin B6-related neurotoxicity. Am J Ther. **29**: e637–e643. 2022. [Medline] [CrossRef]
17. Chua CL, Ohnishi A, Tateishi J, and Kuroiwa Y. Morphometric evaluation of degenerative and regenerative changes in isoniazid-induced neuropathy. Acta Neuropathol. **60**: 183–193. 1983. [Medline] [CrossRef]
18. Ohnishi A, Chua CL, and Kuroiwa Y. Axonal degeneration distal to the site of accumulation of vesicular profiles in the myelinated fiber axon in experimental isoniazid neuropathy. Acta Neuropathol. **67**: 195–200. 1985. [Medline] [CrossRef]
19. Schalaepfer WW, and Hager H. Ultrastructural Studies of INH-induced neuropathy in rats. 1. Early axonal changes. Am J Pathol. **45**: 209–219. 1964. [Medline]
20. Schlaepfer WW, and Hager H. Ultrastructural Studies of INH-induced neuropathy in rats. 3. Repair and regeneration. Am J Pathol. **45**: 679–689. 1964. [Medline]
21. Jacobs JM, Miller RH, and Cavanagh JB. The distribution of degenerative changes in INH neuropathy. Further evidence for focal axonal lesions. Acta Neuropathol. **48**: 1–9. 1979. [Medline] [CrossRef]
22. Arsalan R, and Sabzwari S. Isoniazid induced motor-dominant neuropathy. J Pak Med Assoc. **65**: 1131–1133. 2015. [Medline]
23. Argov Z, and Mastaglia FL. Drug-induced peripheral neuropathies. BMJ. **1**: 663–666. 1979. [Medline] [CrossRef]

24. Aita JF, and Calame TR. Peripheral neuropathy secondary to isoniazid-induced pyridoxine deficiency. Md State Med J. **21**: 68–70. 1972. [Medline]
25. Steichen O, Martinez-Almoyna L, and De Broucker T. [Isoniazid induced neuropathy: consider prevention] (in French). Rev Mal Respir. **23**: 157–160. 2006. [Medline] [CrossRef]
26. Deuis JR, Dvorakova LS, and Vetter I. Methods used to evaluate pain behaviors in rodents. Front Mol Neurosci. **10**: 284. 2017. [Medline] [CrossRef]
27. Mathiasen JR, and Moser VC. The Irwin Test and Functional Observational Battery (FOB) for assessing the effects of compounds on behavior, physiology, and safety pharmacology in rodents. Curr Protoc. **3**: e780. 2023. [Medline] [CrossRef]
28. Ugrenović S, Jovanović I, Vasović L, Kundalić B, Čukuranović R, and Stefanović V. Morphometric analysis of the diameter and g-ratio of the myelinated nerve fibers of the human sciatic nerve during the aging process. Anat Sci Int. **91**: 238–245. 2016. [Medline] [CrossRef]
29. Horai Y, Kakimoto T, Takemoto K, and Tanaka M. Quantitative analysis of histopathological findings using image processing software. J Toxicol Pathol. **30**: 351–358. 2017. [Medline] [CrossRef]
30. Horai Y, Mizukawa M, Nishina H, Nishikawa S, Ono Y, Takemoto K, and Baba N. Quantification of histopathological findings using a novel image analysis platform. J Toxicol Pathol. **32**: 319–327. 2019. [Medline] [CrossRef]
31. Hwang JH, Lim M, Han G, Park H, Kim YB, Park J, Jun SY, Lee J, and Cho JW. A comparative study on the implementation of deep learning algorithms for detection of hepatic necrosis in toxicity studies. Toxicol Res. **39**: 399–408. 2023. [Medline] [CrossRef]
32. Bankhead P. Developing image analysis methods for digital pathology. J Pathol. **257**: 391–402. 2022. [Medline] [CrossRef]
33. Campos SAR, Sanada LS, Sato KL, and Fazan VPS. Morphometry of saphenous nerve in young rats. J Neurosci Methods. **168**: 8–14. 2008. [Medline] [CrossRef]